

1 Functional MRI brain state 2 occupancy in the presence of 3 cerebral small vessel disease – 4 pre-registration for a replication 5 analysis of the Hamburg City Health 6 Study

✉ For correspondence:

e.schlemm@uke.de

Present address:

Dr. Dr. Eckhard Schlemm,
Klinik und Poliklinik für
Neurologie,
Universitätsklinikum
Hamburg-Eppendorf,
Martinistr. 52,
D-20251 Hamburg

Data availability:

Preprocessed data will be
available e.g. on
<https://github.com/csi-hamburg/HCHS-brain-states-RR>.

Funding: Deutsche
Forschungsgemeinschaft
(DFG) – 178316478 – C2

Competing interests: The
author declares no
competing interests.

7 Eckhard Schlemm, MBBS PhD ¹ ✉ and Thies Ingwersen, MD ¹

8 ¹Department of Neurology, University Medical Center
9 Hamburg-Eppendorf

11 Abstract

12 **Objective:** To replicate recent findings about the association between the extent of
13 cerebral small vessel disease (cSVD), functional brain network dedifferentiation and
14 cognitive impairment.

15 **Methods:** We will analyze demographic, imaging and behavioral data from the
16 prospective population-based Hamburg City Health Study. Using a fully prespecified
17 analysis pipeline, we will estimate discrete brain states from structural and resting-state
18 functional magnetic resonance imaging (MRI). In a multiverse analysis we will vary brain
19 parcellations and functional MRI confound regression strategies. Severity of cSVD will
20 be operationalised as the volume of white matter hyperintensities of presumed
21 vascular origin. Processing speed and executive dysfunction are quantified by the trail
22 making test (TMT).

23 **Hypotheses:** We hypothesize a) that greater volume of supratentorial white matter

24 hyperintensities is associated with less time spent in functional MRI-derived brain
25 states of high fractional occupancy; and b) that less time spent in these high-occupancy
26 brain states is associated with longer time to completion in part B of the TMT.

28 Introduction

29 Cerebral small vessel disease (cSVD) is an arteriopathy of the brain, associated with
30 age and common cardiovascular risk factors (Wardlaw, C. Smith, and Dichgans, 2013).
31 cSVD predisposes to ischemic, in particular lacunar, stroke and may lead to cognitive im-
32 pairment and dementia (Cannistraro et al., 2019). Neuroimaging findings in cSVD reflect
33 its underlying pathology (Wardlaw, Valdés Hernández, and Muñoz-Maniega, 2015) and
34 include white matter hyperintensities (WMH) and lacunes of presumed vascular origin,
35 small subcortical infarcts and microbleeds, enlarged perivascular spaces as well as brain
36 atrophy (Wardlaw, E. E. Smith, et al., 2013). However, the extent of visible cSVD features
37 on magnetic resonance imaging (MRI) is an imperfect predictor of the severity of clini-
38 cal sequelae (Das et al., 2019), and our understanding of the causal mechanisms linking
39 cSVD-associated brain damage to clinical deficits remains limited (Bos et al., 2018).

40 Recent efforts have concentrated on exploiting network aspects of the structural (Tu-
41 ladhar, Dijk, et al., 2016; Tuladhar, Tay, et al., 2020; Lawrence, Zeestraten, et al., 2018) and
42 functional (Dey et al., 2016; Schulz et al., 2021) organization of the brain to understand
43 the relation between cSVD and clinical deficits in cognition and other domains reliant
44 on distributed processing. Reduced structural network efficiency has repeatedly been
45 described as a causal factor in the development of cognitive impairment, in particular
46 executive dysfunction and reduced processing speed, in cSVD (Lawrence, Chung, et al.,
47 2014; Shen et al., 2020; Reijmer et al., 2016; Prins et al., 2005). Findings with respect to
48 functional connectivity (FC), on the other hand, are more heterogeneous than their SC
49 counterparts, perhaps because FC measurements are prone to be affected by hemody-
50 namic factors and noise, resulting in relatively low reliability, especially with resting-state
51 scans of short duration (Laumann, Gordon, et al., 2015). This problem is exacerbated
52 in the presence of cSVD and made worse by the arbitrary processing choices (Lawrence,
53 Tozer, et al., 2018; Gesierich et al., 2020).

54 As a promising new avenue, time-varying, or dynamic, functional connectivity approaches
55 have more recently been explored in patients with subcortical ischemic vascular disease

56 (Yin et al., 2022; Xu et al., 2021). While the study of dynamic FC measures may not solve
57 the problem of limited reliability, especially in small populations or subjects with exten-
58 sive structural brain changes, it adds another – temporal – dimension to the study of
59 functional brain organisation, which is otherwise overlooked. Importantly, FC dynamics
60 do not only reflect moment-to-moment fluctuations in cognitive processes but are also
61 related to brain plasticity and homeostasis (Laumann and Snyder, 2021; Laumann, Sny-
62 der, et al., 2017), which may be impaired in cSVD.

63 In the present paper, we aim to replicate and extend the main results of (Schlemm et
64 al., 2022); in this recent study, the authors analyzed MR imaging and clinical data from the
65 prospective Hamburg City Health Study (HCHS, (Jagodzinski et al., 2020)) using a coacti-
66 vation pattern approach to define discrete brain states, and found associations between
67 the WMH load, time spent in high-occupancy brain states characterized by activation or
68 suppression of the default mode network (DMN) and cognitive impairment. Specifically,
69 every 4.7-fold increase in WMH volume was associated with a 0.95-fold reduction of
70 the odds of occupying a DMN-related brain state; every 2.5 seconds (i.e., one repetition
71 time) not spent in one of those states was associated with a 1.06-fold increase of TMT-B
72 completion times.

73 The fractional occupancy of a functional MRI-derived discrete brain state is a subject-
74 specific measure of brain dynamics defined as the proportion of BOLD volumes assigned
75 to that state relative to all BOLD volumes acquired during a resting-state scan.

76 Our primary hypothesis is that the volume of supratentorial white matter hyperinten-
77 sities is associated with the fractional occupancy of DMN-related brain states in a middle-
78 aged to elderly population mildly affected by cSVD. Our ~~second~~-secondary hypothesis is
79 that this fractional occupancy is associated with executive dysfunction and reduced pro-
80 cessing speed, measured as the time to complete part B of the trail making test (TMT).

81 Both hypotheses will be tested in an independent subsample of the HCHS study popu-
82 lation using the same imaging protocols, examination procedures and analysis pipelines
83 as in (Schlemm et al., 2022). The robustness of associations will be explored in a multi-
84 verse approach by varying key steps in the analysis pipeline.

85 **Methods**

Question	Hypothesis	Sampling plan	Analysis plan	Rationale for the sensitivity of the test	Interpretation given different outcomes	Theory that could be shown wrong by the outcome
Is severity of cerebral small disease, quantified by the volume of supratentorial white matter hyperintensities of presumed vascular origin (WMH), associated with time spent in high-occupancy brain states, defined by resting-state functional MRI?	(Primary) Higher WMH volume is associated with lower average occupancy of the two highest-occupancy brain states.	Available subjects with clinical and imaging data from the the HCHS (Jagodzinski et al., 2020)	Standardized pre-processing of structural and functional MRI data • automatic quantification of WMH • co-activation pattern analysis • multivariable generalised regression analyses	Tradition	$P < 0.05 \rightarrow$ rejection of the null hypothesis of no association between cSVD and fractional occupancy; $P > 0.05 \rightarrow$ insufficient evidence to reject the null hypothesis	Functional brain dynamics are not related to subcortical ischemic vascular disease.
Is time spent in high-occupancy brain states associated with cognitive impairment, measured as the time to complete part B of the trail making test (TMT)?	(Secondary) Lower average occupancy of the two highest-occupancy brain states is associated with longer TMT-B time.	as above	as above	as above	$P < 0.05 \rightarrow$ rejection of the null hypothesis of no association between fractional occupancy and cognitive impairment; $P > 0.05 \rightarrow$ insufficient evidence to reject the null hypothesis	Cognitive function is not related to MRI-derived functional brain dynamics.

Table 1. Study Design Template

86 Study population

87 The paper will analyze data from the Hamburg City Health Study (HCHS), which is an
88 ongoing prospective, population-based cohort study aiming to recruit a cross-sectional
89 sample of 45 000 adult participants from the city of Hamburg, Germany (Jagodzinski et al.,
90 2020). From the first 10 000 participants of the HCHS we will aim to include those who
91 were documented to have received brain imaging (n=2652) and exclude those who were
92 analyzed in our previous report (Schlemm et al., 2022) (n=988), for an expected sample
93 size of approximately 1500 participants. The ethical review board of the Landesärztekam-
94 mer Hamburg (State of Hamburg Chamber of Medical Practitioners) approved the HCHS
95 (PV5131), all participants provided written informed consent.

96 Demographic and clinical characterization

97 From the study database we will extract participants' age at the time of inclusion in years,
98 their sex and the number of years spent in education. During the visit at the study cen-
99 ter, participants undergo cognitive assessment using standardized tests. We will extract
100 from the database their performance scores in the Trail Making Test part B, measured
101 in seconds, as an operationalization of executive function and psychomotor processing
102 speed (Tombaugh, 2004; Arbuthnott and Frank, 2000). [For descriptive purposes, we will](#)
103 [also extract data on past medical history and report the proportion of participants with](#)
104 [a previous diagnosis of any dementia.](#)

105 **MRI acquisition and preprocessing**

106 The magnetic resonance imaging protocol for the HCHS includes structural and resting-
107 state functional sequences. The acquisition parameters on a 3 T Siemens Skyra MRI scan-
108 ner (Siemens, Erlangen, Germany) have been reported before (Petersen et al., 2020; Frey
109 et al., 2021) and are given as follows:

110 For T_1 -weighted anatomical images, a 3D rapid acquisition gradient-echo sequence
111 (MPRAGE) was used with the following sequence parameters: repetition time TR = 2500 ms,
112 echo time TE = 2.12 ms, 256 axial slices, slice thickness ST = 0.94 mm, and in-plane resolu-
113 tion IPR = (0.83×0.83) mm².

114 T_2 -weighted fluid attenuated inversion recovery (FLAIR) images were acquired with
115 the following sequence parameters: TR = 4700 ms, TE = 392 ms, 192 axial slices, ST =
116 0.9 mm, IPR = (0.75×0.75) mm².

117 125 resting state functional MRI volumes were acquired (TR = 2500 ms; TE = 25 ms;
118 flip angle = 90°; slices = 49; ST = 3 mm; slice gap = 0 mm; IPR = (2.66×2.66) mm²). Subjects
119 were asked to keep their eyes open and to think of nothing.

120 We will verify the presence and voxel-dimensions of expected MRI data for each par-
121 ticipant and exclude those for whom at least one of T_1 -weighted, FLAIR and resting-state
122 MRI is missing. We will also exclude participants with a neuroradiologically confirmed
123 space-occupying intra-axial lesion. To ensure reproducibility, no visual quality assess-
124 ment on raw images will be performed.

125 For the remaining participants, structural and resting-state functional MRI data will
126 be preprocessed using FreeSurfer v6.0 (<https://surfer.nmr.mgh.harvard.edu/>), and fmriPrep
127 v20.2.6 (Esteban et al., 2019), using default parameters. Participants will be excluded if
128 automated processing using at least one of these packages fails.

129 **Quantification of WMH load**

130 For our primary analysis, the extent of ischemic white matter disease will be operational-
131 ized as the total volume of supratentorial WMHs obtained from automated segmentation
132 using a combination of anatomical priors, BIANCA (Griffanti, Zamboni, et al., 2016) and
133 LOCATE (Sundaresan et al., 2019), post-processed with a minimum cluster size of 30 vox-
134 els, as described in (Schlemm et al., 2022). In an exploratory analysis, we partition voxels
135 identified as WMH into deep and periventricular components according to their distance
136 to the ventricular system (cut-off 10 mm, (Griffanti, Jenkinson, et al., 2018))

137 **Brain state estimation**

138 Output from fMRIPrep will be post-processed using xcpEngine v1.2.1 to obtain de-confounded
139 spatially averaged BOLD time series (Circic, Wolf, et al., 2017). For the primary analysis we
140 will use the *36p* regression strategy and the Schaefer-400 parcellation (Schaefer et al.,
141 2018), as in (Schlemm et al., 2022).

142 Different atlases and confound regression strategies, as implemented in xcpEngine,
143 will be included in the exploratory multiverse analysis.

144 Co-activation pattern (CAP) analysis will be performed by first aggregating parcellated,
145 de-confounded BOLD signals into a $(n_{\text{parcels}} \times \sum_i n_{\text{time points},i})$ feature matrix, where $n_{\text{time points},i}$
146 denotes the number of retained volumes for subject i after confound regression. Cluster-
147 ing will be performed using the k -means algorithm ($k = 5$) with distance measure given
148 by 1 minus the sample Pearson correlation between points, as implemented in Matlab
149 R2021a. We will estimate subject- and state-specific fractional occupancies, which are
150 defined as the proportion of BOLD volumes assigned to each brain state (Vidaurre et al.,
151 2018). The two states with the highest average occupancy will be identified as the basis
152 for further analysis.

153 **Statistical analysis**

154 For demographic (age, sex, years of education) and clinical (TMT-B) variables the number
155 of missing records will be reported. For non-missing values, we will provide descriptive
156 summary statistics using median and interquartile range. The proportion of men and
157 women in the sample will be reported. ~~Regression~~ Since we expect, based on our pilot
158 data (Schlemm et al., 2022), that the proportion of missing data will be small, regression
159 modelling will be carried out as a complete-case analysis.

160 As a first outcome-neutral quality check of the implementation of the MRI process-
161 ing pipeline, brain state estimation and co-activation pattern analysis, we will compare
162 fractional occupancies between brain states. We expect that the average fractional oc-
163 cupancy in two high-occupancy states is higher than the average fractional occupancy in
164 the other three states. Point estimates and 95% confidence intervals will be presented
165 for the difference in average fractional occupancy to check this assertion.

166 For further analyses, non-zero WMH volumes will be subjected to a logarithmic trans-
167 formation. Zero values will retain their value zero; to compensate, all models will include
168 a binary indicator for zero WMH volume if at least one non-zero value is present.

169 To assess the primary hypothesis of a negative association between the extent of is-
170 chemic white matter disease and time spent in high-occupancy brain states, we will per-
171 form a fixed-dispersion beta-regression to model the logit of the conditional expectation
172 of the average fractional occupancy of two high-occupancy states as an affine function
173 of the logarithmized WMH load. Age and sex will be included as covariates. The strength
174 of the association will be quantified as an odds ratio per interquartile ratio of the WMH
175 burden distribution and accompanied by a 95% confidence interval. Significance testing
176 of the null hypothesis of no association will be conducted at the conventional significance
177 level of 0.05. Estimation and testing will be carried out using the 'betareg' package v3.1.4
178 in R v4.2.1.

179 To assess the secondary hypothesis of an association between time spent in high-
180 occupancy brain states and executive dysfunction, we will perform a generalized linear
181 regression with a Gamma response distribution to model the logarithm of the condi-
182 tional expected completion time in part B of the TMT as an affine function of the average
183 fractional occupancy of two high-occupancy states. Age, sex, years of education and log-
184 arithmized WMH load will be included as covariates. The strength of the association will
185 be quantified as a multiplicative factor per percentage point and accompanied by a 95%
186 confidence interval. Significance testing of the null hypothesis of no association will be
187 conducted at the conventional significance level of 0.05. Estimation and testing will be
188 carried out using the glm function included in the 'stats' package from R v4.2.1.

189 Sample size calculation is based on an effect size on the odds ratio scale of 0.95, corre-
190 sponding to an absolute difference in the probability of occupying a DMN-related brain
191 state between the first and third WMH-load quartile of 1.3 percentage points, and be-
192 tween the 5% and 95% percentile of 3.1 percentage points. Approximating half the dif-
193 ference in fractional occupancy of DMN-related states between different task demands
194 (rest vs n-back) in healthy subjects, which was estimated to lie between 6 and 7 percent-
195 age points (Cornblath et al., 2020), this value represent a plausible choice for the smallest
196 effect size of theoretical and practical interest. It also equals the effect size estimated
197 based on the data presented in (Schlemm et al., 2022).

198 We used simple bootstrapping to create 10 000 hypothetical datasets of size 200, 400,
199 600, 800, 900, 910, ..., 1100, 1200, 1400, 1500, 1600. Each dataset was subjected to the esti-
200 mation procedure described above. For each sample size, the proportion of datasets in
201 which the primary null hypothesis of no association between fractional occupancy and

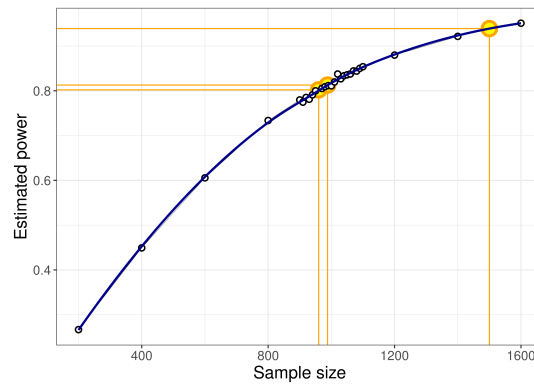


Figure 1. Estimated power for different sample sizes is obtained as the proportion of synthetic data sets in which the null hypothesis of no association between WMH volume and time spent in high-occupancy brain states can be rejected at the $\alpha = 0.05$ significance level. Proportions are based on a total of 10 000 synthetic data sets obtained by bootstrapping the data presented in (Schlemm et al., 2022). Highlighted in orange are the smallest sample size ensuring a power of at least 80 % ($n = 960$), the sample size of the pilot data ($n = 988$, post-hoc power 81.3 %), and the expected sample size for this replication study ($n = 1500$, a-priori power 93.9 %).

202 WMH load could be rejected at $\alpha = 0.05$ was computed and is recorded as a power curve
 203 in Figure 1.

204 It is seen that a sample size of 960 would allow replication of the reported effect with
 205 a power of 80.2 %. We anticipate a sample size of 1500, which yields a power of 93.9 %.

206 Multiverse analysis

207 Both in (Schlemm et al., 2022) and for our primary replication analysis we made certain
 208 analytical choices in the operationalization of brain states and ischemic white matter
 209 disease, namely the use of the $36p$ confound regression strategy, the Schaefer-400 par-
 210 cellation and a BIANCA/LOCATE-based WMH segmentation algorithm. The robustness
 211 of the association between WMH burden and time spent in high-occupancy states with
 212 regard to other choices will be explored in a multiverse analysis (Steege et al., 2016).
 213 Specifically, in an exploratory analysis, we will estimate brain states from BOLD time se-
 214 ries processed according to a variety of established confound regression strategies and
 215 aggregated over different cortical brain parcellations (Table 2, Ciric, Rosen, et al., 2018;
 216 Ciric, Wolf, et al., 2017). Extent of cSVD will additionally be quantified by the volume of
 217 deep and periventricular white matter hyperintensities.

218 For each combination of analytical choice of confound regression strategy, parcella-
 219 tion and subdivision of white matter lesion load ($9 \times 9 \times 3 = 243$ scenarios in total) we will
 220 quantify the association between WMH load and average time spent in high-occupancy
 221 brain states using odds ratio and 95 % confidence intervals as described above.

Name of the atlas	#parcels	Reference	Design	Reference
Desikan-Killiany	86	Desikan et al., 2006	24p	Friston et al., 1996
AAL	116	Tzourio-Mazoyer et al., 2002	24p + GSR	Macey et al., 2004
Harvard-Oxford	112	Makris et al., 2006	36p	Satterthwaite et al., 2013
glasser360	360	Glasser et al., 2016	36p + spike regression	Cox, 1996
gordon333	333	Gordon et al., 2016	36p + despiking	Satterthwaite et al., 2013
power264	264	Power, Cohen, et al., 2011	36p + scrubbing	Power, Mitra, et al., 2014
schaefer{N}	100	Schaefer et al., 2018	aCompCor	Muschelli et al., 2014
	200		tCompCor	Behzadi et al., 2007
	400		AROMA	Pruim et al., 2015

AAL: Automatic Anatomical Labelling

(a) Parcellations

GSR: Global signal regression, AROMA: Automatic Removal of Motion Artifacts

(b) Confound regression strategies, adapted from (Ciric, Wolf, et al., 2017)

Table 2. Multiverse analysis, implemented using xcpEngine (Ciric, Rosen, et al., 2018)

222 No hypothesis testing and will be carried out in these multiverse analyses. They rather
 223 serve to inform about the robustness of the outcome of the test of the primary hypothe-
 224 sis. Any substantial conclusions about the association between severity of cerebral small
 225 pathology and time spent in high-occupancy brain states, as stated in the Scientific Ques-
 226 tion in Table 1, will be drawn from the primary analysis using pre-specified methodolog-
 227 ical choices.

228 Further exploratory analysis

229 In previous work, two high-occupancy brain states were related to the default-mode net-
 230 work (Cornblath et al., 2020). We will further explore this relation by computing, for each
 231 individual brain state, the cosine similarity of the positive and negative activations of
 232 the cluster’s centroid with a set of a-priori defined functional ‘communities’ or networks
 233 (Schaefer et al., 2018; Yeo et al., 2011). Results will be thus visualized as spider plots for
 234 the Schaefer, Gordon and Power atlases.

235 In further exploratory analyses we plan to describe the associations between brain
 236 state dynamics and other measures of cognitive ability, such as memory and language.

237 Code and pilot data

238 Summary data from the first 1000 imaging data points of the HCHS have been published
 239 with (Schlemm et al., 2022) and form the basis for the hypotheses tested in this replication
 240 study. We have implemented our prespecified analysis pipeline described above in R
 241 and Matlab, and applied it to this previous sample. Data, code and results have been
 242 stored on GitHub (https://github.com/csi-hamburg/HCHS_brain_states_RR) und preserved
 243 on Zenodo.

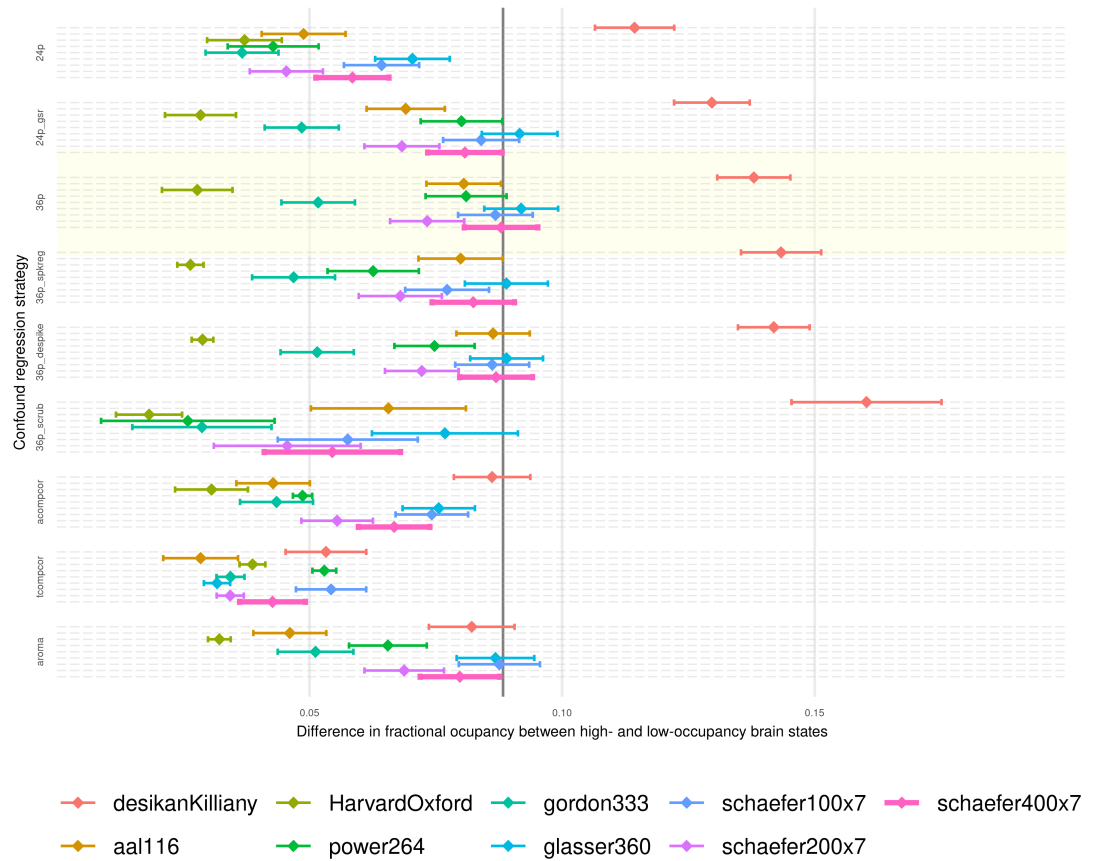


Figure 2. Point estimates (dots) and 95 % confidence intervals (line segments) for the mean difference in fractional occupancy between high- and low occupancy states are shown for different confound regression strategies (groups along the vertical axis) and brain parcellations (color). The difference in FO for a particular choice of regression strategy and brain parcellation is nominally statistically significantly different from zero at a significance level of 5% if the corresponding interval does not contain zero. Hence, the FO difference is significant for *all* processing choices, reflecting the separation between high- and low-occupancy states. The primary choices (*36p* and *schaefer400*) are highlighted by a yellow box and thick pink line, respectively. The effect size reported in (Schlemm et al., 2022) is indicated by a vertical line at 0.08830623.

244 Thus re-analysing data from 988 subjects, the separation between two high-occupancy
 245 and three low-occupancy brain states could be reproduced for all combinations of brain
 246 parcellation and confound regression strategies (Figure 2).

247 In a multiverse analysis, the main finding was somewhat robust with respect to these
 248 choices: a statistically significant negative association between WMH load and time spent
 249 in high-occupancy states was observed in 18/81 scenarios, with 5/81 statistically signifi-
 250 cant positive associations occurring with the Desikan–Killiany parcellation only (Figure 3).

251 The secondary finding of an association between greater TMT-B times and lower frac-
 252 tional occupancy was similarly robust with 12/81 statistically significant negative and no

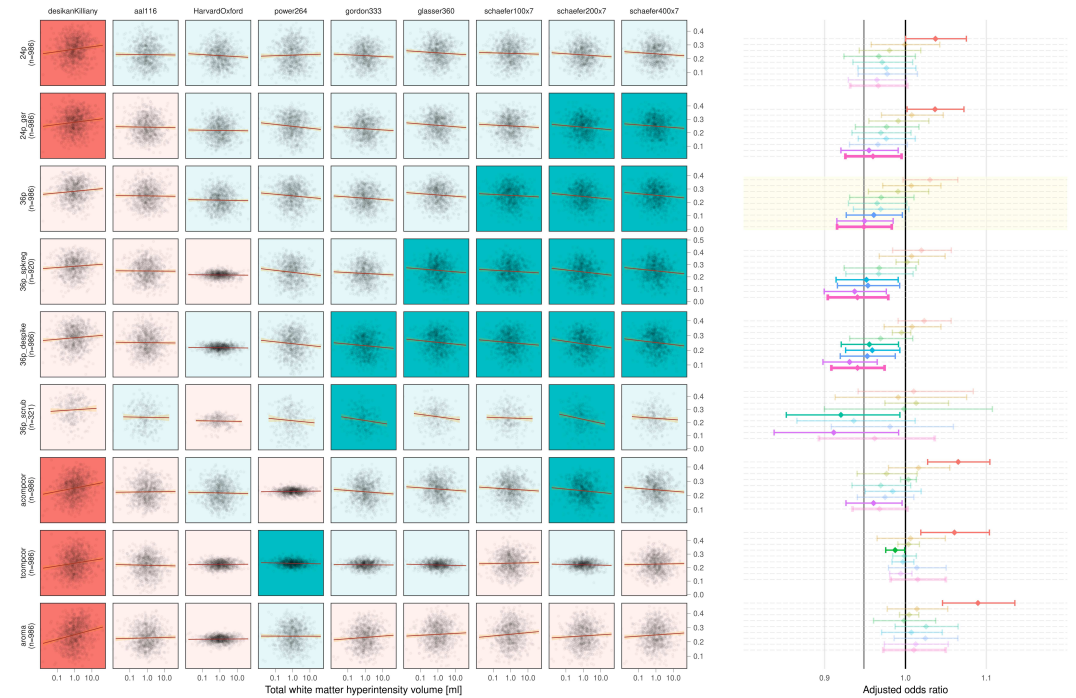



Figure 3. On the left, scatter plots of average fractional occupancies in high-occupancy states against WMH volume on a logarithmic scale (base 10 for easier visualization) for different combinations of confound regression strategies and brain parcellations. Linear regression lines indicate the direction of the unadjusted association between $\log(\text{WMH})$ and occupancy. Background color of individual panels indicates the direction of the association after adjustment for age, sex and zero WMH volume (green, negative; red, positive). A pale background indicates that the association between $\log(\text{WMH})$ and average occupancy is not statistically different from zero. On the right, the same information is shown using point estimates and 95 % confidence intervals for the adjusted odds ratio of the association.

253 statistically significant positive associations.

254 **Timeline and access to data**

255 At the time of planning of this study, all demographic, clinical and imaging data used in
256 this analysis have been collected by the HCHS and are held in the central trial database.
257 Quality checks for non-imaging variables have been performed centrally. WMH segmen-
258 tation based on structural MRI data of the first 10 000 participants of the HCHS has been
259 performed previously using the BIANCA/LOCATE approach (Rimmele et al., 2022) and re-
260 sults are included in this preregistration (`./derivatives/WMH/cSVD_a11.csv`). Functional
261 MRI data and clinical measures of executive dysfunction (TMT-B scores) have not been
262 analyzed by the author. Analysis of the data will begin immediately after acceptance-in-
263 principle of the stage 1 submission of the registered report is obtained. Submission of
264 the full manuscript (stage 2) is planned two months later.

265 **Acknowledgment**

266 This preprint was created using the LaPreprint template ([https://github.com/roaldarbol/](https://github.com/roaldarbol/lapreprint)
267 [lapreprint](https://github.com/roaldarbol/lapreprint)) by Mikkel Roald-Arbøl .

268 **References**

- 269 Arbuthnott, Katherine and Janis Frank (2000). "Trail making test, part B as a measure of
270 executive control: validation using a set-switching paradigm". In: *Journal of clinical and*
271 *experimental neuropsychology* 22.4, pp. 518–528.
- 272 Behzadi, Yashar et al. (2007). "A component based noise correction method (CompCor)
273 for BOLD and perfusion based fMRI". In: *Neuroimage* 37.1, pp. 90–101.
- 274 Bos, Daniel et al. (2018). "Cerebral small vessel disease and the risk of dementia: A sys-
275 tematic review and meta-analysis of population-based evidence". en. In: *Alzheimers.*
276 *Dement.* 14.11, pp. 1482–1492.
- 277 Cannistraro, Rocco J et al. (2019). "CNS small vessel disease: A clinical review". en. In: *Neu-*
278 *rology* 92.24, pp. 1146–1156.
- 279 Ciric, Rastko, Adon FG Rosen, et al. (2018). "Mitigating head motion artifact in functional
280 connectivity MRI". In: *Nature protocols* 13.12, pp. 2801–2826.
- 281 Ciric, Rastko, Daniel H Wolf, et al. (2017). "Benchmarking of participant-level confound
282 regression strategies for the control of motion artifact in studies of functional con-
283 nectivity". en. In: *Neuroimage* 154, pp. 174–187.

- 284 Cornblath, Eli J et al. (2020). "Temporal sequences of brain activity at rest are constrained
285 by white matter structure and modulated by cognitive demands". en. In: *Commun Biol*
286 3.1, p. 261.
- 287 Cox, Robert W (1996). "AFNI: software for analysis and visualization of functional mag-
288 netic resonance neuroimages". In: *Computers and Biomedical research* 29.3, pp. 162-
289 173.
- 290 Das, Alvin S et al. (2019). "Asymptomatic Cerebral Small Vessel Disease: Insights from
291 Population-Based Studies". en. In: *J. Stroke Cerebrovasc. Dis.* 21.2, pp. 121-138.
- 292 Desikan, Rahul S et al. (2006). "An automated labeling system for subdividing the human
293 cerebral cortex on MRI scans into gyral based regions of interest". In: *Neuroimage* 31.3,
294 pp. 968-980.
- 295 Dey, Ayan K et al. (2016). "Pathoconnectomics of cognitive impairment in small vessel
296 disease: A systematic review". en. In: *Alzheimers. Dement.* 12.7, pp. 831-845.
- 297 Esteban, Oscar et al. (2019). "fMRIPrep: a robust preprocessing pipeline for functional
298 MRI". en. In: *Nat. Methods* 16.1, pp. 111-116.
- 299 Frey, Benedikt M et al. (2021). "White matter integrity and structural brain network topol-
300 ogy in cerebral small vessel disease: The Hamburg city health study". en. In: *Hum. Brain*
301 *Mapp.* 42.5, pp. 1406-1415.
- 302 Friston, Karl J et al. (1996). "Movement-related effects in fMRI time-series". In: *Magnetic*
303 *resonance in medicine* 35.3, pp. 346-355.
- 304 Gesierich, Benno et al. (2020). "Alterations and test-retest reliability of functional connec-
305 tivity network measures in cerebral small vessel disease". en. In: *Hum. Brain Mapp.*
306 41.10, pp. 2629-2641.
- 307 Glasser, Matthew F et al. (2016). "A multi-modal parcellation of human cerebral cortex".
308 en. In: *Nature* 536.7615, pp. 171-178.
- 309 Gordon, Evan M et al. (2016). "Generation and Evaluation of a Cortical Area Parcellation
310 from Resting-State Correlations". en. In: *Cereb. Cortex* 26.1, pp. 288-303.
- 311 Griffanti, Ludovica, Mark Jenkinson, et al. (2018). "Classification and characterization of
312 periventricular and deep white matter hyperintensities on MRI: A study in older adults".
313 en. In: *Neuroimage* 170, pp. 174-181.
- 314 Griffanti, Ludovica, Giovanna Zamboni, et al. (2016). "BIANCA (Brain Intensity AbNormal-
315 ity Classification Algorithm): A new tool for automated segmentation of white matter
316 hyperintensities". en. In: *Neuroimage* 141, pp. 191-205.

317 Jagodzinski, Annika et al. (2020). "Rationale and Design of the Hamburg City Health Study".
318 en. In: *Eur. J. Epidemiol.* 35.2, pp. 169–181.

319 Laumann, Timothy O, Evan M Gordon, et al. (2015). "Functional system and areal organi-
320 zation of a highly sampled individual human brain". In: *Neuron* 87.3, pp. 657–670.

321 Laumann, Timothy O and Abraham Z Snyder (2021). "Brain activity is not only for thinking".
322 In: *Current Opinion in Behavioral Sciences* 40, pp. 130–136.

323 Laumann, Timothy O, Abraham Z Snyder, et al. (2017). "On the stability of BOLD fMRI
324 correlations". In: *Cerebral cortex* 27.10, pp. 4719–4732.

325 Lawrence, Andrew J, Ai Wern Chung, et al. (2014). "Structural network efficiency is as-
326 sociated with cognitive impairment in small-vessel disease". en. In: *Neurology* 83.4,
327 pp. 304–311.

328 Lawrence, Andrew J, Daniel J Tozer, et al. (2018). "A comparison of functional and trac-
329 tography based networks in cerebral small vessel disease". en. In: *Neuroimage Clin* 18,
330 pp. 425–432.

331 Lawrence, Andrew J, Eva A Zeestraten, et al. (2018). "Longitudinal decline in structural
332 networks predicts dementia in cerebral small vessel disease". en. In: *Neurology* 90.21,
333 e1898–e1910.

334 Macey, Paul M et al. (2004). "A method for removal of global effects from fMRI time series".
335 In: *Neuroimage* 22.1, pp. 360–366.

336 Makris, Nikos et al. (2006). "Decreased volume of left and total anterior insular lobule in
337 schizophrenia". In: *Schizophrenia research* 83.2-3, pp. 155–171.

338 Muschelli, John et al. (2014). "Reduction of motion-related artifacts in resting state fMRI
339 using aCompCor". In: *Neuroimage* 96, pp. 22–35.

340 Petersen, Marvin et al. (2020). "Network Localisation of White Matter Damage in Cerebral
341 Small Vessel Disease". en. In: *Sci. Rep.* 10.1, p. 9210.

342 Power, Jonathan D, Alexander L Cohen, et al. (2011). "Functional network organization of
343 the human brain". en. In: *Neuron* 72.4, pp. 665–678.

344 Power, Jonathan D, Anish Mitra, et al. (2014). "Methods to detect, characterize, and re-
345 move motion artifact in resting state fMRI". In: *Neuroimage* 84, pp. 320–341.

346 Prins, Niels D et al. (2005). "Cerebral small-vessel disease and decline in information pro-
347 cessing speed, executive function and memory". en. In: *Brain* 128.Pt 9, pp. 2034–2041.

348 Pruijm, Raimon HR et al. (2015). "ICA-AROMA: A robust ICA-based strategy for removing
349 motion artifacts from fMRI data". In: *Neuroimage* 112, pp. 267–277.

350 Reijmer, Yael D et al. (2016). "Small vessel disease and cognitive impairment: The rele-
351 vance of central network connections". en. In: *Hum. Brain Mapp.* 37.7, pp. 2446–2454.
352 Rimmele, David Leander et al. (2022). "Association of Carotid Plaque and Flow Velocity
353 With White Matter Integrity in a Middle-aged to Elderly Population". en. In: *Neurology*.
354 Satterthwaite, Theodore D et al. (2013). "An improved framework for confound regres-
355 sion and filtering for control of motion artifact in the preprocessing of resting-state
356 functional connectivity data". In: *Neuroimage* 64, pp. 240–256.
357 Schaefer, Alexander et al. (2018). "Local-Global Parcellation of the Human Cerebral Cortex
358 from Intrinsic Functional Connectivity MRI". en. In: *Cereb. Cortex* 28.9, pp. 3095–3114.
359 Schlemm, Eckhard et al. (2022). "Equalization of Brain State Occupancy Accompanies
360 Cognitive Impairment in Cerebral Small Vessel Disease". en. In: *Biol. Psychiatry* 92.7,
361 pp. 592–602.
362 Schulz, Maximilian et al. (2021). "Functional connectivity changes in cerebral small vessel
363 disease - a systematic review of the resting-state MRI literature". en. In: *BMC Med.* 19.1,
364 p. 103.
365 Shen, Jun et al. (2020). "Network Efficiency Mediates the Relationship Between Vascular
366 Burden and Cognitive Impairment: A Diffusion Tensor Imaging Study in UK Biobank".
367 en. In: *Stroke* 51.6, pp. 1682–1689.
368 Steegen, Sara et al. (2016). "Increasing Transparency Through a Multiverse Analysis". en.
369 In: *Perspect. Psychol. Sci.* 11.5, pp. 702–712.
370 Sundaesan, Vaanathi et al. (2019). "Automated lesion segmentation with BIANCA: Im-
371 pact of population-level features, classification algorithm and locally adaptive thresh-
372 olding". en. In: *Neuroimage* 202, p. 116056.
373 Tombaugh, Tom N (2004). "Trail Making Test A and B: normative data stratified by age
374 and education". en. In: *Arch. Clin. Neuropsychol.* 19.2, pp. 203–214.
375 Tuladhar, Anil M, Ewoud van Dijk, et al. (2016). "Structural network connectivity and cog-
376 nition in cerebral small vessel disease". en. In: *Hum. Brain Mapp.* 37.1, pp. 300–310.
377 Tuladhar, Anil M, Jonathan Tay, et al. (2020). "Structural network changes in cerebral small
378 vessel disease". en. In: *J. Neurol. Neurosurg. Psychiatry* 91.2, pp. 196–203.
379 Tzourio-Mazoyer, Nathalie et al. (2002). "Automated anatomical labeling of activations in
380 SPM using a macroscopic anatomical parcellation of the MNI MRI single-subject brain".
381 In: *Neuroimage* 15.1, pp. 273–289.

382 Vidaurre, Diego et al. (2018). "Discovering dynamic brain networks from big data in rest
383 and task". en. In: *Neuroimage* 180.Pt B, pp. 646–656.

384 Wardlaw, Joanna M, Colin Smith, and Martin Dichgans (2013). "Mechanisms of sporadic
385 cerebral small vessel disease: insights from neuroimaging". en. In: *Lancet Neurol.* 12.5,
386 pp. 483–497.

387 Wardlaw, Joanna M, Eric E Smith, et al. (2013). "Neuroimaging standards for research
388 into small vessel disease and its contribution to ageing and neurodegeneration". en.
389 In: *Lancet Neurol.* 12.8, pp. 822–838.

390 Wardlaw, Joanna M, Maria C Valdés Hernández, and Susana Muñoz-Maniega (2015). "What
391 are white matter hyperintensities made of? Relevance to vascular cognitive impair-
392 ment". en. In: *J. Am. Heart Assoc.* 4.6, p. 001140.

393 Xu, Yuanhang et al. (2021). "Altered Dynamic Functional Connectivity in Subcortical Is-
394 chemic Vascular Disease With Cognitive Impairment". en. In: *Front. Aging Neurosci.* 13,
395 p. 758137.

396 Yeo, B T Thomas et al. (2011). "The organization of the human cerebral cortex estimated
397 by intrinsic functional connectivity". en. In: *J. Neurophysiol.* 106.3, pp. 1125–1165.

398 Yin, Wenwen et al. (2022). "The Clustering Analysis of Time Properties in Patients With
399 Cerebral Small Vessel Disease: A Dynamic Connectivity Study". en. In: *Front. Neurol.*
400 13, p. 913241.